Mineralogical Magazine (2022), **86**, 141–149
doi:10.1180/mgm.2021.104

CAMBRIDGE UNIVERSITY PRESS

Article

Illoqite-(Ce), $Na_2NaBaCeZnSi_6O_{17}$, a new member of the nordite supergroup from Ilímaussaq alkaline complex, South Greenland.

Emil H. Gulbransen[1]*, Henrik Friis[1], Fabrice Dal Bo[1] and Muriel Erambert[2]

[1]Natural History Museum, University of Oslo, P.O. Box 1172, Blindern, 0318 Oslo, Norway; and [2]Department of Geoscience, University of Oslo, P.O. Box 1047, Blindern, 0316 Oslo, Norway

Abstract

The new mineral, illoqite-(Ce), with the ideal formula $Na_2NaBaCeZnSi_6O_{17}$, has been discovered in the Taseq Slope, Ilímaussaq Alkaline Complex, Southern Greenland. Illoqite-(Ce) occurs in a hyperalkaline ussingite vein closely related to one of the largest ussingite veins in the Ilímaussaq complex. The associated minerals are aegirine, arfvedsonite, a britholite-group mineral, epistolite, chkalovite, lueshite, Mn-rich pectolite group member and steenstrupine-(Ce). Illoqite-(Ce) crystallises as either single euhedral crystals up to 150 μm in size or radiating aggregates consisting of a few or many crystals. The aggregates are up to 200 μm in diameter. Illoqite-(Ce) can occur as scattered small groups of crystals or aggregates, but sometimes they occur in high concentrations creating clusters or bands almost completely consisting of illoqite-(Ce). The empirical formula on the basis of 17 anions is $Na_{2.00}Na_{1.00}(Ba_{0.59}Sr_{0.32}Ca_{0.04}Na_{0.03})_{\Sigma 0.98}(Ce_{0.68}La_{0.31}Nd_{0.09}Pr_{0.04})_{\Sigma 1.12}(Zn_{0.42}Fe_{0.34}Li_{0.14}Mn_{0.09})_{\Sigma 0.99}Si_{5.97}O_{17}$, with the simplified formula being $Na_2Na(Ba,Sr)(Ce,La,Nd)(Zn,Fe,Li)Si_6O_{17}$. Illoqite-(Ce) exhibits sector zoning between elements Sr and Ba. The crystal structure was determined using single-crystal X-ray diffraction data and refined to $R_1 = 2.46\%$ using 1902 unique reflections. Illoqite-(Ce) is orthorhombic, *Pcca*, with $a = 14.5340(7)$, $b = 5.2213(1)$, $c = 19.8270(4)$ Å, $V = 1507.25(6)$ Å^3 and $Z = 4$. The strongest lines of the powder X-ray diffraction pattern [*d*, Å (*I*, %) (*hkl*)] are: 7.266 (79) (200), 4.688 (44) (104), 4.241 (64) (210), 3.486 (79) (114), 3.340 (52) (312), 2.986 (67) (410), 2.882 (100) (314) and 2.789 (44) (016). Illoqite-(Ce) is a new member of the nordite supergroup and is named after the Greenlandic word illoq, meaning cousin, in allusion to the mineral's close relation to nordite-(Ce).

Keywords: illoqite-(Ce), new mineral, nordite supergroup, Ilímaussaq Alkaline Complex, crystal structure, *REE*-minerals, sector zoning

(Received 21 October 2021; accepted 22 December 2021; Accepted Manuscript published online: 28 January 2022; Associate Editor: Ferdinando Bosi)

Introduction

The new mineral, illoqite-(Ce), with the ideal formula $Na_2NaBaCeZnSi_6O_{17}$, has been discovered in the Taseq Slope, Ilímaussaq Alkaline Complex, Southern Greenland. The Ilímaussaq alkaline complex is exposed in a 136 km^2 large area that stretches across the Tunulliarfik and Kangerluarsuk fjords in the Gardar Province of Southern Greenland (Fig. 1). More than 230 different mineral species are described from Ilímaussaq, it being the type locality for 35 of those, including illoqite-(Ce).

The new mineral is named after the Greenlandic word illoq which means cousin, and describes the relation between illoqite-(Ce) and the nordite supergroup (Dal Bo *et al.*, 2021). As Ce is the dominant *REE*, the name has a suffix in accordance with Bayliss and Levinson (1988) for naming *REE* minerals. Illoqite-(Ce) is the sixth member of the nordite group of minerals with the general formula $A_2BXYZT_6O_{17}$, where $^{[6-8]}$A = Na; $^{[6]}$B = Na, Ca; $^{[8]}$X = Ca, Sr, Ba; $^{[8]}$Y = REE^{3+}; $^{[4]}$Z = Mg, Mn^{2+} Fe^{2+}, Zn and $^{[4]}$T = Si (Tables 1 and 2). The new mineral and name (symbol Ilq-Ce) were approved by the Commission on New Minerals, Nomenclature and Classification of the International Mineralogical Association (IMA2021-021, Gulbransen *et al.*, 2021). The type material is deposited in the mineralogical collections of the Natural History Museum, University of Oslo, NHM Økern, Kabelgata 38–40, 0580 Oslo, Norway, with catalogue numbers KNR 44274 and KNR 44275.

Occurrence and paragenesis

The geology of the Ilímaussaq complex is well described in the literature (Ussing, 1912; Larsen and Sørensen, 1987; Sørensen and Larsen, 1987, 2001; Upton, 2013). The Gardar Province went through a series of continental rifts, alkaline magmatism and sedimentation 1300–1140 Ma. The province is separated into the two major periods of volcanic activity called Older Gardar (1300–1163 M.y.) and Younger Gardar (1163–1140 M.y.). A review of age determination of Ilímaussaq, including a new age of 1156 ± 1.4 Ma, is provided by Borst *et al.* (2019). The Mesoproterozoic igneous Ilímaussaq complex was formed during late magmatism along the southern rift zone

***Author for correspondence:** Emil H. Gulbransen, Email: e.h.gulbransen@nhm.uio.no
Cite this article: Gulbransen E.H., Friis H., Dal Bo F. and Erambert M. (2022) Illoqite-(Ce), $Na_2NaBaCeZnSi_6O_{17}$, a new member of the nordite supergroup from Ilímaussaq alkaline complex, South Greenland.. *Mineralogical Magazine* **86**, 141–149. https://doi.org/10.1180/mgm.2021.104

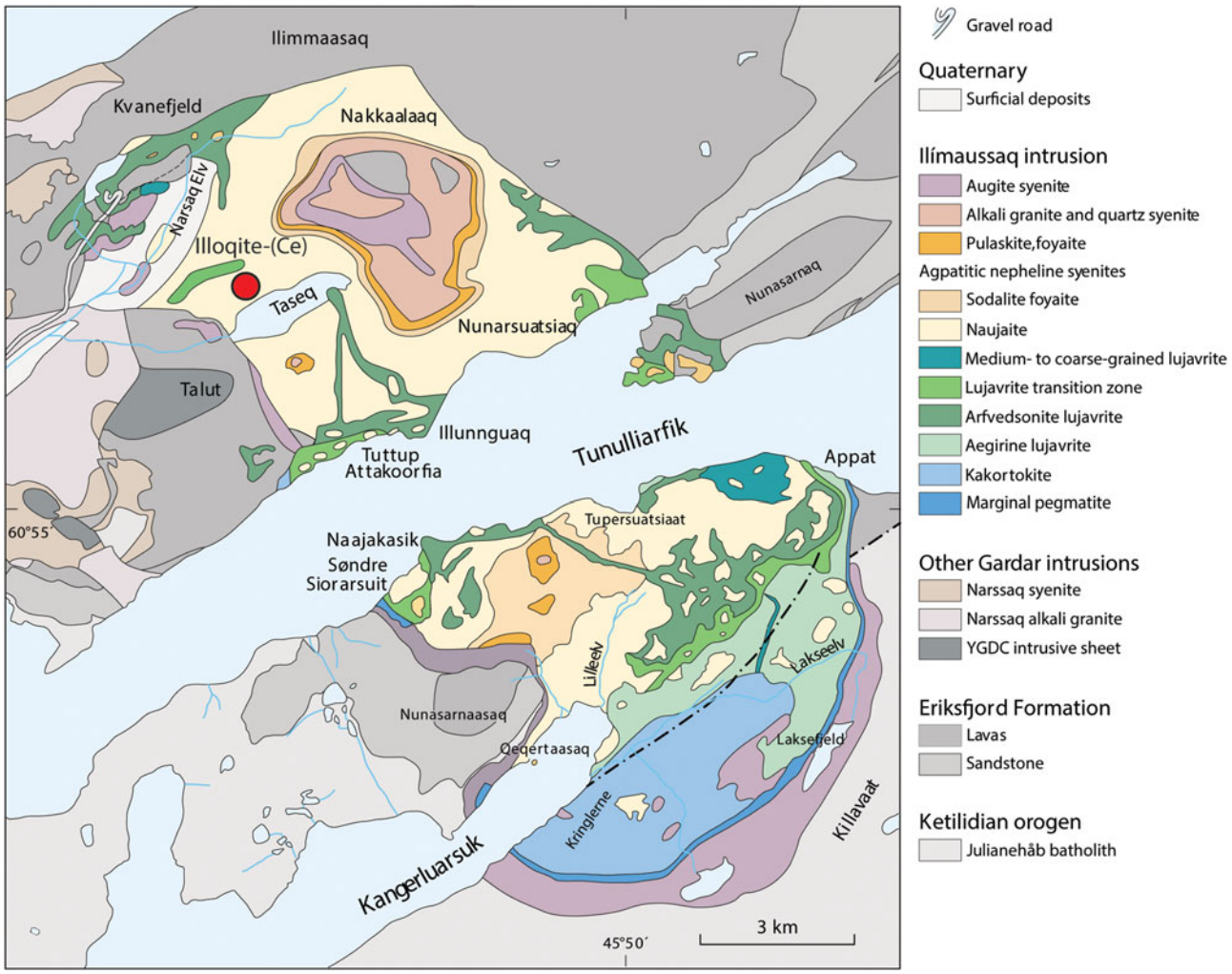

Fig. 1. Geological map of the Ilímaussaq alkaline complex. Modified from Upton (2013), showing the illoqite-(Ce) locality on the Taseq slope.

and marks the end of the magmatism in the Gardar Province (Upton, 2013).

The Taseq Slope is situated in the northern part of Ilímaussaq and predominantly consists of naujaite. Naujaite is a cumulate rock consisting of greyish to greenish euhedral sodalite enclosed in alkali-feldspar, black to dark-green arfvedsonite and aegirine, and red eudialyte. The naujaite exhibits a poikilitic texture due to the early formation of cumulus sodalite in the magma chamber, which floated to the top of the magma chamber. The eudialyte content can vary a lot as also seen in the kakortokites, however the magmatic layering is not as pronounced in the naujaites. In addition to the naujaites, a more evolved rock, lujavrite is also common on the Taseq slope. This hyperagpaitic rock is the youngest of the nepheline syenites, consisting of the same felsic mineralogy, i.e. nepheline, albite, microcline and sodalite. There are several varieties of lujavrites in the complex, with both textural and mineralogical differences. However, the two main lujavrites can be separated by colour based on which mafic mineral is present in the rock: black (arfvedsonite) and green (aegirine) (Ussing, 1912; Upton, 2013; Friis, 2015). Illoqite-(Ce) was discovered in loose boulders by a large ussingite vein on the Taseq Slope in the Ilímaussaq alkaline complex. The initial sample was collected by one of the authors (HF) in 2014. Additional material was collected in the summer of 2019. Despite searching the area no samples were found *in situ*, therefore it is not possible to establish where in the ussingite vein the mineral formed.

Illoqite-(Ce) is only the sixth Ba-mineral to be described from Ilímaussaq after barylite, ilímaussite-(Ce), joaquinite-(Ce), kuannersuite-(Ce) and ortho-joaquinite-(La) (Petersen, 2001). All of these minerals are rare in Ilímaussaq, however ilímaussite-(Ce) has its type locality on the Taseq slope and the large ussingite vein is where most of this mineral has been found (Fig. 1). One theory to why we find two Ba-rich minerals here is that due to the size of the ussingite vein, any incompatible element not fitting the structure of ussingite or the other main minerals will have to form discrete species. Alongside ussingite as a matrix mineral, aegirine and arfvedsonite occur as major components. Furthermore, the paragenesis of illoqite-(Ce) consists of britholite-(Ce), ancylite-(Ce), epistolite, chkalovite, lueshite, steenstrupine-(Ce) and polylithionite, where ancylite-(Ce) is the brownish weathering product of illoqite-(Ce) (Fig. 2).

The abundance of chkalovite (Fig. 2) lead Engel *et al.* (1971) to conduct a Be-mineralisation study of the Taseq slope. The study produced some detailed maps over its geology and mineralogy (Fig. 3). The origin of the ussingite veins is not fully understood but they could be classified as hydrothermalites, believed to be a primary, but late, stage in the alkaline rock forming process involving extreme alkaline hydrothermal fluids

Table 1. List of the valid nordite supergroup minerals and their unit-cell parameters.

Mineral species		*a* (Å)	*b* (Å)	*c* (Å)	Space group	*Z*	References
Nordite group							
Nordite-(La)	$Na_3SrLaZnSi_6O_{17}$	14.468(8)	5.203(6)	19.88(2)	*Pcca*	4	[1–3*]
Nordite-(Ce)	$Na_3SrCeZnSi_6O_{17}$	14.389(1)	5.180(1)	19.755(1)	*Pcca*	4	[4–5*]
Ferronordite-(La)	$Na_3SrLaFeSi_6O_{17}$	14.440(5)	5.191(2)	19.86(1)	*Pcca*	4	[6]
Ferronordite-(Ce)	$Na_3SrCeFeSi_6O_{17}$	14.46(1)	5.194(3)	19.874(9)	*Pcca*	4	[7–8*]
Manganonordite-(Ce)	$Na_3SrCeMnSi_6O_{17}$	14.44(2)	5.187(5)	19.82(1)	*Pcca*	4	[7–8*]
Illoqite-(Ce)	$Na_3BaCeZnSi_6O_{17}$	14.5596(4)	5.2213(1)	19.8270(4)	*Pcca*	4	[9]
Unassigned member							
Meieranite	$Na_2Sr_3MgSi_6O_{17}$	7.938(1)	10.492(1)	18.256(1)	$P2_1nb$	4	[10]

*Unit-cell parameters are taken from this reference.
References: [1] Gerasmovsky (1941); [2] Bakakin *et al.* (1970); [3] Sokolova *et al.* (1992); [4] Semenov (1961); [5] Dal Bo *et al.* (2021); [6] Pekov *et al.* (2001); [7] Pekov *et al.* (1998); [8] Pushcharovskii *et al.* (1999); [9] this study; [10] Yang *et al.* (2019).

Table 2. Cationic distribution in the crystal structure of the approved end-members of the nordite supergroup.

	A	A'	B	X	Y	Z	T	O
Nordite group								
Nordite-(La)	Na_2		Na	Sr	La	Zn	Si_6	O_{17}
Nordite-(Ce)	Na_2		Na	Sr	Ce	Zn	Si_6	O_{17}
Ferronordite-(La)	Na_2		Na	Sr	La	Fe	Si_6	O_{17}
Ferronordite-(Ce)	Na_2		Na	Sr	Ce	Fe	Si_6	O_{17}
Manganonordite-(Ce)	Na_2		Na	Sr	Ce	Mn	Si_6	O_{17}
Illoqite-(Ce)	Na_2		Na	Ba	Ce	Zn	Si_6	O_{17}
Unassigned member								
Meieranite	Na	Sr	Na	Sr	Sr	Mg	Si_6	O_{17}

(Khomyakov, 1995). Consequently, the ussingite veins, and illoqite-(Ce), should be considered formed by primary magmatic processes rather than traditional later hydrothermal alteration events.

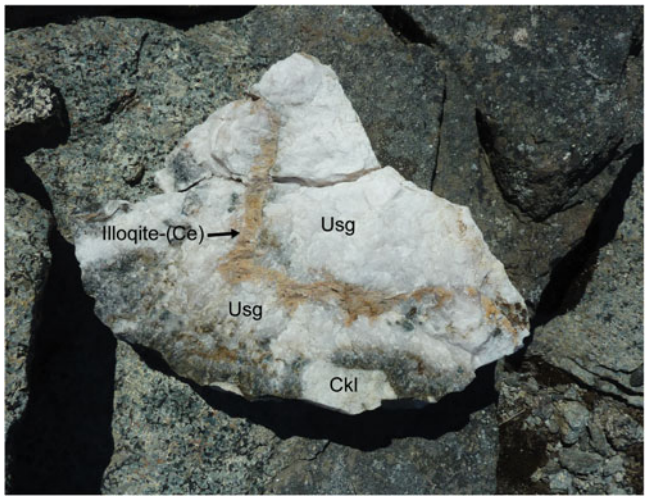

Fig. 2. Example of the paragenesis of illoqite-(Ce) with the brown 'band' running through the rock being weathered illoqite-(Ce). Ussingite (Usg) and chkalovite (Ckl) are marked respectively.

Physical properties

Illoqite-(Ce) occurs as either single euhedral crystals up to 150 μm in size or radiating aggregates consisting of a few or many crystals. The aggregates are up to 200 μm in diameter (Fig. 4). Illoqite-(Ce) can occur as scattered small groups of crystals or aggregates, but sometimes they occur in high concentrations creating clusters or bands consisting almost completely of illoqite-(Ce) (Fig. 2). However, illoqite-(Ce) is always intergrown with ussingite. The colour of illoqite-(Ce) is pink in daylight, but brownish yellow under fluorescent light and some halogen lights. It shows no photoluminescence under either long-wave or short-wave ultraviolet light. Most of the physical properties could not be determined due to small grain size and intergrowths with ussingite, but the mineral appears dull and the powder colour is white with a faint yellow tint. The calculated density based on the empirical formula and refined unit cell parameters is 3.65(3) g/cm^3. For the above mentioned reasons and the chemical zonation (Fig. 5), optical properties were only determined from the thin section used for chemical characterisation. The birefringence was determined to be ~0.021, which is in good agreement with the published values for nordite minerals ranging between 0.019 and 0.023 (Gerasimovsky, 1941; Pekov *et al.* 1998, 2001). To estimate $n_{av.}$ we used the Gladstone–Dale compatibility index and by assuming the range of Superior and Excellent, we find $n_{av.}$ to be between 1.626 and 1.651 (Mandarino, 1981). The range is consistent with the published values for nordites $n_{av.} = 1.632–1.635$ (Gerasimovsky, 1941; Pekov *et al.* 1998, 2001), and using the Becke line method showing that $n_{av.}$ of illoqite-(Ce) is between those of ussingite (1.519) and arfvedsonite (1.682).

Chemistry

The quantitative chemical data were collected using an electron microprobe CAMECA XS100 equipped with five wavelength dispersive spectrometers housed at the Department of Geosciences, University of Oslo. X-ray lines and spectrometer diffracting crystals used for analysis were selected to minimise interference between *REE* and between Ba–Ce, and an overlap correction procedure applied to correct the interference of Zn*L*β on Na*K*α. Matrix effects were corrected using the PAP procedure (Pouchou and Pichoir, 1984). The analytical conditions during collection were the following: wavelength dispersive mode, accelerating voltage of 15 kV; beam current of 15 nA; beam diameter of 5 μm and number of analyses of 15. The standards used for calibration were wollastonite (Si*K*α and Ca*K*α), metallic Fe (Fe*K*α), albite (Na*K*α), synthetic MgO (Mg*K*α), pyrophanite (Mn*K*α), ZnS (Zn*L*α), $BaSO_4$ (Ba*L*α), Sr-SiO glass (Sr*L*α) and 'synthetic *REE* orthophosphates' (La*L*α, Ce*L*β, Pr*L*β and Nd*L*β)

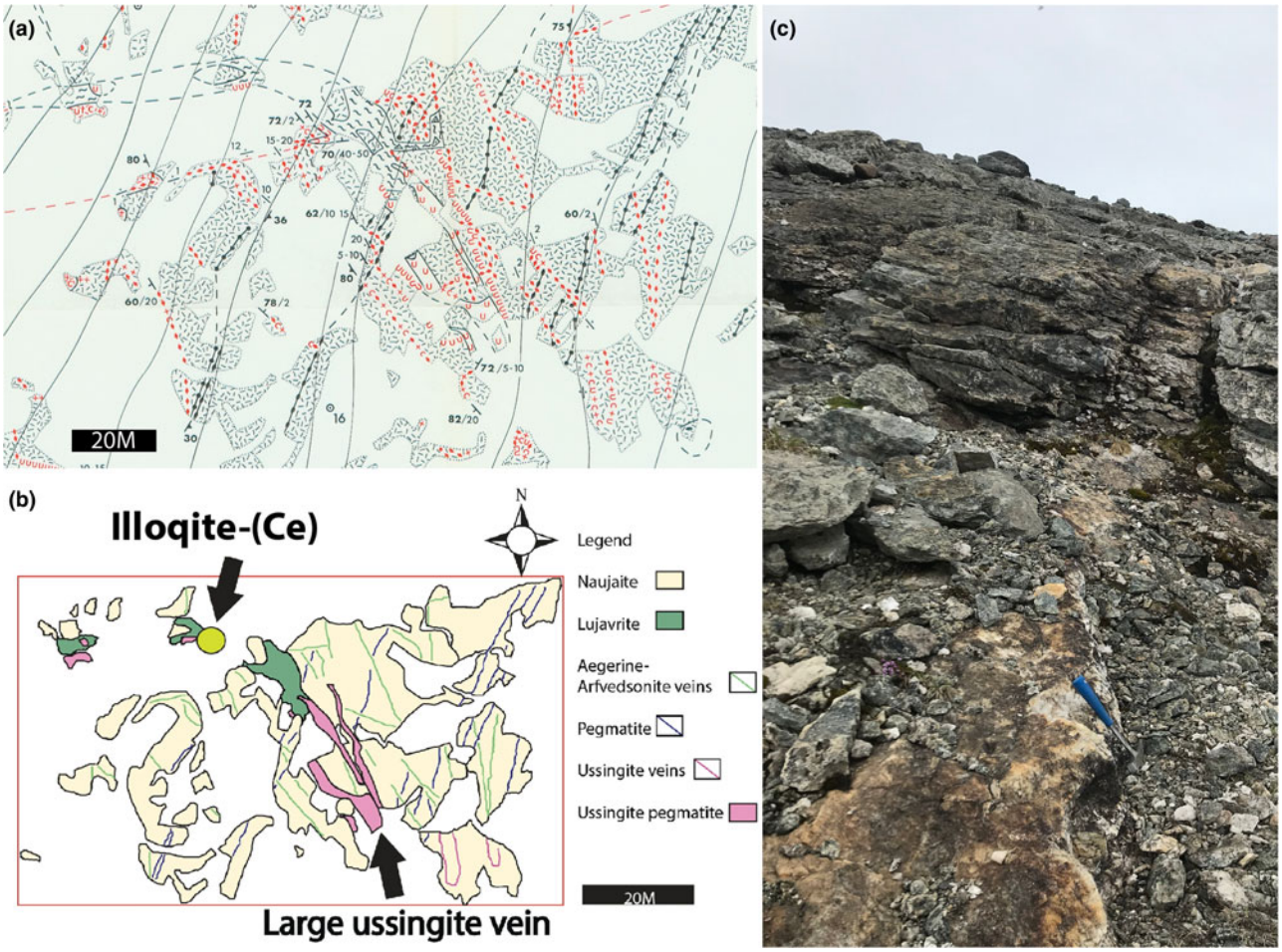

Fig. 3. Illoqite-(Ce) locality at the Taseq slope. (a) Detailed geological map modified from Engell *et al.* (1971). (b) Highlighted geological map of (a), including the location of the illoqite-(Ce) occurrence. The vein is sloping with decreasing altitude towards the northwest. (c) Picture of the large ussingite close to the illoqite-(Ce) occurrence. Geological hammer as scale.

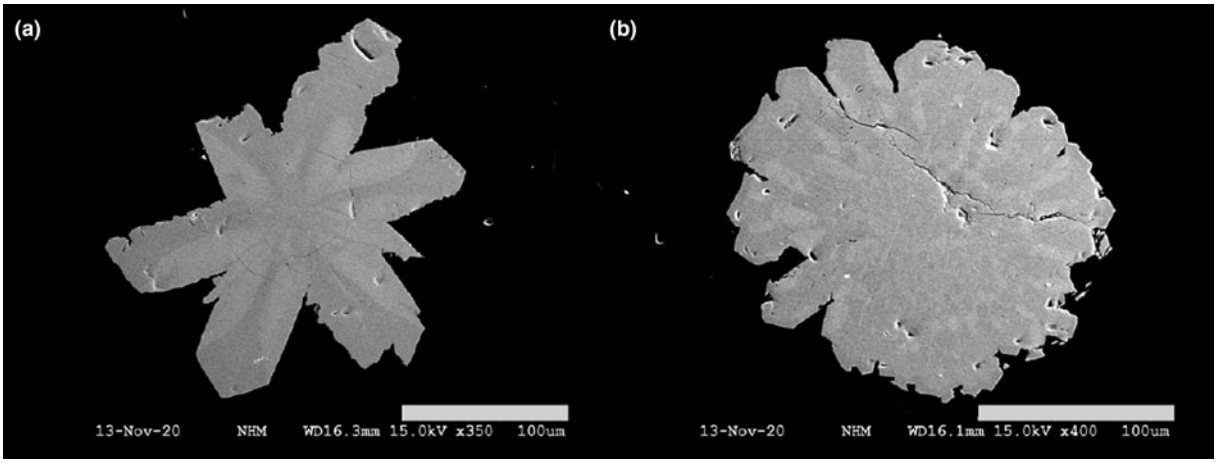

Fig. 4. Back-scattered electron images of two illoqite-(Ce) aggregates in ussingite showing the chemical heterogeneity (both images from sample KNR 44274). In both images the scale bar is 100 μm.

obtained from the Smithsonian Institution, Washington D.C (Jarosewich and Boatner, 1991).

To get quantitative values on Li the epoxy mount used for electron probe micro-analyser (EPMA) was analysed on a Bruker Aurora Elite quadrupole laser ablation inductively coupled plasma mass spectrometry (LA-ICP-MS) equipped with a 213 nm CTAC laser housed at the Department of Geoscience, University of Oslo. NIST 610 was used for instrument calibration and to monitor

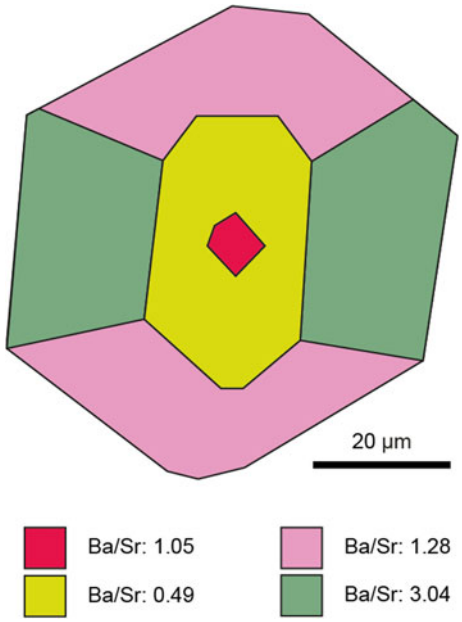

Fig. 5. Schematic drawing of typical sector zoning in illoqite-(Ce) with the Ba/Sr ratio given for each zone. Note: Some crystals may have compositional zones like nordite-(Ce).

Table 3. Chemical electron microprobe data (in wt.%) for illoqite-(Ce).

Constituent	Mean	Range	S.D.	Calibration standards
SiO_2	43.04	42.27–44.02	1.12	Wollastonite
La_2O_3	6.00	4.14–6.65	1.19	Orthophosphate#
Ce_2O_3	13.49	12.53–14.41	0.98	Orthophosphate#
Pr_2O_3	0.87	0.64–1.26	0.36	Orthophosphate#
Nd_2O_3	1.84	1.37–3.15	1.06	Orthophosphate#
BaO	10.80	4.43–13.31	5.75	$BaSO_4$
SrO	3.94	2.69–7.41	3.02	Sr–Si-glass
CaO	0.25	0.04–0.51	0.20	Wollastonite
ZnO	4.08	3.69–4.94	0.78	Sphalerite
MnO	0.78	0.63–0.92	0.17	Pyrophanite
FeO	2.97	2.15–3.38	0.68	Pure metal
Na_2O	11.28	10.92–11.90	0.57	Albite
Li_2O*	0.25			
Total	99.59			

S.D. = standard deviation (2σ); *From LA-ICP-MS; #Jarosewich and Boatner (1991).

drift during experiments. Silicon measured on EPMA was used as internal standard and the data were processed using the *Glitter* program (Griffin *et al.* 2008). The chemical compositions of illoqite-(Ce) are given in Table 3.

Based on the recent approved nordite supergroup nomenclature (Dal Bo *et al.*, 2021), the empirical formula of illoqite-(Ce) calculated on the basis of 17 anions is: $Na_{2.00}Na_{1.00}(Ba_{0.59}Sr_{0.32}Ca_{0.04}Na_{0.03})_{\Sigma 0.98}(Ce_{0.68}La_{0.31}Nd_{0.09}Pr_{0.04})_{\Sigma 1.12}(Zn_{0.42}Fe_{0.34}Li_{0.14}Mn_{0.09})_{\Sigma 0.99}Si_{5.97}O_{17}$. The simplified formula is: $Na_2Na(Ba,Sr)(Ce,La,Nd)(Zn,Fe,Li)Si_6O_{17}$, while the ideal formula is: $Na_2NaBaCeZnSi_6O_{17}$, which requires Na_2O 10.91; BaO 17.99; Ce_2O_3 19.26; ZnO 9.55 and SiO_2 42.30; total 100 (wt.% oxide). The ideal formula is derived from the empirical formula using the IMA dominant-constituent rule (Hatert and Burke, 2008). The chemical variation in particular of Sr and Ba (Table 3) is the result of pronounced sector zoning (Figs 4 and 5). The individual zones are smaller than the diameter of the laser used and too small to separate for single-crystal X-ray diffraction (SXRD). To keep consistency between the average results of the SXRD data we have decided to use the average composition including the various zones, and not just the one with highest Ba content. Pekov (2000) mentioned that it is possible to find zonal nordite with the Z-site occupants varying from Mn dominant, Fe dominant and Zn dominant. This is similar to illoqite-(Ce) though the X-site determines the zonation rather than the Z-site occupants.

Table 4. Experimental and calculated* powder X-ray diffraction data (*d* in Å) for illoqite-(Ce).

I_{meas}	d_{meas}	I_{calc}	d_{calc}	*h k l*	I_{meas}	d_{meas}	I_{calc}	d_{calc}	*h k l*
79	**7.266**	71	7.279	2 0 0	8	1.886	3	1.887	5 0 8
20	4.945	6	4.956	0 0 4	29	1.777	21	1.785	4 2 6
44	**4.688**	35	4.692	1 0 4			6	1.783	1 2 8
30	4.389	16	4.403	1 1 2			21	1.777	6 2 0
64	**4.241**	50	4.242	2 1 0	17	1.730	6	1.733	6 0 8
26	3.608	5	3.594	0 1 4			14	1.731	3 1 10
79	**3.486**	65	3.490	1 1 4	5	1.692	1	1.693	8 1 2
52	**3.340**	51	3.346	3 1 2			2	1.692	2 3 0
23	3.222	11	3.223	2 1 4	5	1.650	3	1.652	0 0 12
67	**2.986**	26	3.009	2 0 6			1	1.651	4 1 10
		66	2.985	4 1 0	6	1.631	7	1.631	1 3 4
100	**2.882**	100	2.888	3 1 4	12	1.561	9	1.563	5 1 10
44	**2.789**	44	2.792	0 1 6	12	1.555	13	1.555	3 3 4
20	2.607	20	2.610	0 2 0	8	1.500	5	1.501	3 2 10
12	2.555	11	2.557	4 1 4	9	1.495	2	1.496	4 3 4
		1	2.548	1 2 1			6	1.492	8 2 0
6	2.513	5	2.510	5 0 4	8	1.472	10	1.475	9 1 4
32	2.439	31	2.446	4 0 6	6	1.457	3	1.457	5 3 3
		6	2.443	1 0 8	6	1.443	3	1.444	6 2 8
		3	2.438	2 2 1	6	1.427	3	1.430	5 3 4
14	2.423	18	2.426	6 0 0	3	1.398	5	1.402	10 1 0
17	2.350	9	2.355	2 1 7	3	1.389	3	1.390	2 0 14
		2	2.246	2 0 8	11	1.382	10	1.383	7 1 10
17	2.261	17	2.262	5 1 4	5	1.365	3	1.366	0 1 14
8	2.212	3	2.215	4 1 6	9	1.358	2	1.359	7 2 8
		1	2.212	3 1 7			3	1.359	3 0 14
14	2.118	12	2.121	4 2 0	5	1.342	1	1.343	2 1 14
17	2.082	13	2.085	3 2 4	6	1.322	1	1.322	7 3 2
36	2.044	15	2.048	0 2 6	6	1.319	4	1.319	4 0 14
9	2.008	1	2.011	6 1 4	6	1.300	6	1.302	1 3 10
		2	2.010	1 1 9			5	1.300	6 3 6
15	1.959	14	1.971	2 2 6	3	1.263	4	1.262	3 3 10
		3	1.964	1 0 10	5	1.258	1	1.257	8 3 0
		8	1.955	6 0 6			3	1.257	7 2 10
11	1.914	9	1.917	7 0 4					

*The calculated values were obtained using *VESTA 3* (Momma and Izumi, 2011).
The strongest values are given in bold.

Crystallography

Powder X-ray diffraction data were collected on the same fragment as the structure solution using the Gandolfi movement of a Rigaku Synergy-S diffractometer housed at the Natural History Museum in Oslo equipped with a HyPix-6000He detector and Cu*K*α radiation (50 kV and 1 mA). Table 4 presents the observed and calculated powder diffraction data based on the structure model described below. The unit cell parameters were refined in an orthorhombic setting based on 32 reflections using the program *UnitCell* (Holland and Redfern, 1997) and are: $a = 14.5340(7)$, $b = 5.2191(2)$, $c = 19.8121(8)$ Å and $V = 1502.84(7)$ Å^3.

Single-crystal X-ray intensity data were collected at room temperature with monochromated Mo*K*α radiation (50 kV and 1 mA). The instrument has Kappa geometry and both data

Table 5. Data collection and structure refinement details for illoqite-(Ce).

Crystal data	
Ideal structural formula	$Na_2NaBaCeZnSi_6O_{17}$
Temperature (K)	293(2)
Cell setting	Orthorhombic
Space group	*Pcca* (No. 54)
a (Å)	14.5596(4)
b (Å)	5.2213(1)
c (Å)	19.8270(4)
V (Å^3)	1507.25(6)
Z	4
Calculated density (g cm^{-3})	3.65(3)
Crystal size (mm)	0.059 × 0.024 × 0.013
Crystal form	Prismatic
Crystal colour	Pinkish
Data collection	
Diffractometer	Rigaku XtaLAB Synergy, HyPix Detector
Radiation; λ (Å)	Mo*K*α; 0.71073
Absorption coefficient, μ (mm^{-1})	7.957
F(000)	1544
θ range (°)	2.054–31.455
Index range	$-20 < h < 19$, $-7 < k < 7$, $-27 < l < 28$
No. of measured reflections	29,642
Total reflections (N_{tot}) /unique (N_{ref})	2362 / 1902
Criterion for observed reflections	$I > 2\sigma(I)$
Refinement	
Refinement on	Full-matrix least squares on F^2
R, *wR* ($I > 2\sigma(I)$)	2.46, 3.48
R_2, wR_2 (all reflection)	6.28, 6.65
R_{int} (%)	3.96
No. of refinement param. (N_{par})	140
Weight scheme*	$1/(\sigma^2(F_o)^2+0.0355(P)^2+1.8002(P))$
$\Delta\rho_{max}$, $\Delta\rho_{min}$ (e^- Å^{-3})	−1.69 / 1.72
GoF (obs/all)	1.07/1.07

*$P = ((F_o)^2 + 2(F_c)^2)/3)$

Table 6. Site population, atomic coordinates and equivalent isotropic displacement parameters (Å^2) for illoqite-(Ce).

Site	Site population	*x*	*y*	*z*	U_{eq}/U_{iso}
A	$Na_{0.98}Ca_{0.02}$	0.0671(1)	0.5104(2)	0.67249(5)	0.0284(5)
B	$Na_{1.00}$	0	½	½	0.0254(6)
X	$Ba_{0.59}Sr_{0.31}REE_{0.10}$	¼	½	0.52469(2)	0.01285(9)
Y	$REE_{1.00}$	¼	½	0.31864(2)	0.01166(8)
Z	$Zn_{0.42}Fe_{0.34}Li_{0.14}Mn_{0.10}$	¼	0	0.6170(2)	0.0131(2)
T1	Si	0.09574(6)	0.9682(1)	0.56596(4)	0.0126(2)
T2	Si	0.10168(5)	0.9586(1)	0.27464(4)	0.0122(2)
T3	Si	0.11097(5)	0.0472(1)	0.41845(3)	0.0122(2)
O1	O	0.0058(1)	0.1639(4)	0.41777(9)	0.0166(4)
O2	O	0.1677(1)	0.8119(4)	0.61105(9)	0.0182(4)
O3	O	0.1176(1)	0.8681(4)	0.48678(8)	0.0160(4)
O4	O	0.0966(1)	0.2701(4)	0.56955(9)	0.0192(4)
O5	O	0	0.8590(5)	¼	0.0182(6)
O6	O	0.1759(1)	0.7864(4)	0.23411(9)	0.0160(4)
O7	O	0.1169(1)	0.8506(4)	0.35351(8)	0.0153(4)
O8	O	0.1154(1)	0.2591(4)	0.27178(9)	0.0192(4)
O9	O	0.1846(1)	0.2710(4)	0.41598(9)	0.0177(4)

Table 7. Anisotropic atomic displacement parameters (Å^2) for illoqite-(Ce).

Site	U^{11}	U^{22}	U^{33}	U^{12}	U^{13}	U^{23}
A	0.049(1)	0.0208(7)	0.0157(6)	0.0009(4)	−0.0041(5)	−0.0031(6)
B	0.031(1)	0.0174(9)	0.0274(11)	−0.0038(7)	−0.0137(8)	0.0019(7)
X	0.0134(1)	0.0135(1)	0.01166(14)	0.000	0.000	0.00012(9)
Y	0.0129(1)	0.0124(1)	0.00959(11)	0.000	0.000	−0.00056(8)
Z	0.0135(3)	0.0172(3)	0.0085(3)	0.000	0.000	0.0006(2)
T1	0.0145(4)	0.0129(3)	0.0103(3)	0.0011(2)	−0.0002(3)	−0.0009(3)
T2	0.0130(4)	0.0130(3)	0.0107(3)	0.0001(2)	−0.0008(2)	−0.0007(3)
T3	0.0137(4)	0.0139(3)	0.0089(3)	−0.0003(2)	0.0003(2)	−0.0007(3)
O1	0.0165(9)	0.0171(9)	0.0161(9)	0.0001(7)	0.0011(7)	−0.0006(7)
O2	0.021(1)	0.019(1)	0.0146(9)	0.0024(7)	−0.0047(8)	−0.0022(8)
O3	0.021(1)	0.0172(9)	0.0096(8)	0.0015(7)	0.0005(7)	−0.0002(8)
O4	0.026(1)	0.015(1)	0.0162(9)	−0.0009(7)	−0.0018(8)	−0.0022(8)
O5	0.013(1)	0.017(1)	0.0237(14)	0.000	−0.005(1)	0.000
O6	0.017(1)	0.0176(9)	0.0135(8)	0.0006(7)	0.0013(7)	0.0013(8)
O7	0.021(1)	0.0155(9)	0.0092(8)	−0.0003(7)	−0.0001(7)	0.0011(8)
O8	0.024(1)	0.0151(9)	0.0178(9)	0.0026(7)	−0.0036(8)	−0.0029(8)
O9	0.018(1)	0.019(1)	0.0156(9)	0.0009(7)	−0.0001(8)	−0.0043(8)

Table 8. Cationic distribution in the crystal structure of illoqite-(Ce) and nordite-(Ce).

Site	RSS (e^-)	Site-population (apfu)	CSS (e^-)	ABL (Å)	CBL (Å)
Illoqite-(Ce)					
$^{[7]}$A	11.6	$Na_{0.98}Ca_{0.02}$	11.2	2.615	2.529
$^{[6]}$B	10.7	$Na_{1.00}$	11.0	2.430	2.420
$^{[8]}$X	50.2	$Ba_{0.59}Sr_{0.31}REE_{0.10}$	50.6	2.701	2.763
$^{[8]}$Y	57.1	$REE_{1.00}$	58.0	2.554	2.563
$^{[4]}$Z	26.7	$Zn_{0.42}Fe_{0.34}Li_{0.14}Mn_{0.10}$	24.4	1.973	1.995
Nordite-(Ce)[1]					
$^{[7]}$A	11.0	$Na_{1.00}$	11.0	2.602	2.530
$^{[6]}$B	11.0	$Na_{1.00}$	11.0	2.417	2.420
$^{[8]}$X	35.8	$Sr_{0.75}Ca_{0.20}Ba_{0.05}$	35.3	2.620	2.660
$^{[8]}$Y	56.5	$REE_{1.00}$	58.0	2.521	2.563
$^{[4]}$Z	28.9	$Zn_{0.95}Fe_{0.02}Mg_{0.02}Mn_{0.01}$	29.5	1.951	1.981

RSS: Refined site scattering factor, these values are based on the refined site occupancies in Table 6; apfu: atoms per formula unit; CSS: Calculated site scattering factor; ABL: average observed bond-lengths; CBL: calculated bond-lengths; Ideal bond-distances are calculated using the ionic radii of Shannon (1976). Ce^{3+} is used as a proxy for all *REE*. [1]Dal Bo *et al.* (2021)

collection and subsequent data reduction together with face based absorption corrections were carried out using the *CrysAlisPro* software (Rigaku Oxford Diffraction, UK). It was not possible to separate a single domain, due to the chemical heterogenity of the mineral for all the crystals tested. To get a better separation of data from different domains the sample-to-detector distance was 50 mm. We chose the data collection where the main component was more than 90% of the total observed reflections and used the main component data for the structure description. The structure was solved by direct methods using *SHELXS* and refined by *SHELXL* (Sheldrick, 2008) using neutral atom scattering factors and the *WinGX* interface (Farrugia, 2012). Once all atoms were located, they were refined anisotropically and the occupancies were refined freely for the main cations (A = B = Na and Y = Ce). The mixed occupancies Ba *vs* Sr and Zn *vs* Fe were refined at the *X* and *Z*-sites, respectively. See Table 5 for details of data collection and refinement. Atom coordinates, anisotropic atomic displacement parameters and site occupancies are given in Tables 6–8, respectively. The crystallographic information file has been deposited with the Principal Editor of *Mineralogical Magazine* and is available as Supplementary material (see below).

Illoqite-(Ce) is isostructural with the other members of the nordite group, and has a structure based on 12-periodic chains consisting of tetrahedrally coordinated Si (T-sites) that are interconnected via tetrahedrally coordinated Zn (Z-site) creating a sheet perpendicular to the *b* axis (Fig. 6). Adjacent sheets of tetrahedra are separated by a heteropolyhedral layer containing the A (Na), B (Na), X (Ba) and Y (*REE*) sites which are interconnected by edge and face sharing (Fig. 6). The B-site has an octahedral

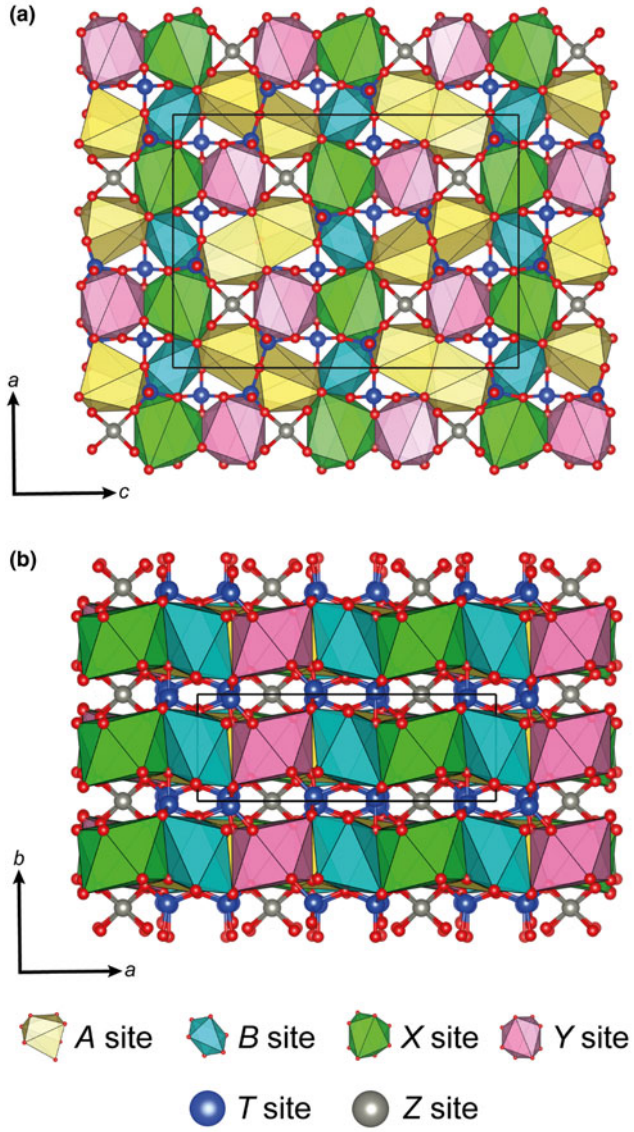

Fig. 6. General view of the crystal structure of illoqite-(Ce) along [010] (a) and [001] (b). The oxygen atoms are represented by red spheres and the solid lines show one unit cell.

Table 9. Selected bond distances (*d in* Å) for illoqite-(Ce).

A–O1	2.687(3)	X–O2 ×2	2.649(2)
A–O2	2.472(2)	X–O3 ×2	2.824(2)
A–O4	2.434(3)	X–O4 ×2	2.687(3)
A–O5	2.653(3)	X–O9 ×2	2.643(2)
A–O6	2.530(3)	<X–O>	2.701
A–O8	2.412(3)		
A–O8	3.119(3)	Y–O6 ×2	2.492(2)
<A–O>	2.615	Y–O7 ×2	2.754(2)
		Y–O8 ×2	2.507(3)
B–O1 ×2	2.397(2)	Y–O9 ×2	2.462(2)
B–O3 ×2	2.587(3)	<Y–O>	2.554
B–O4 ×2	2.306(3)		
<B–O>	2.430	T1–O1	1.663(3)
		T1–O2	1.601(3)
Z–O2 ×2	1.961(2)	T1–O3	1.685(2)
Z–O6 ×2	1.985(2)	T1–O4	1.578(3)
<Z–O>	1.973	<T1–O>	1.632
T2–O5	1.643(1)	T3–O1	1.648(3)
T2–O6	1.619(3)	T3–O3	1.649(2)
T2–O7	1.677(2)	T3–O7	1.649(3)
T2–O8	1.583(3)	T3–O9	1.586(3)
<T2–O>	1.630	<T3–O>	1.633

coordination, whereas the A-site occupants have six bonds between 2.412 and 2.687 Å and one long bond to O8 at 3.119 Å, making it seven coordinated (Table 9). The O7 is at a distance of 3.316 Å from A, but this only contributes 0.02 valence units to the bond and therefore we considered the coordination to be 7-coordinated (Table 10). However, with a different composition the A-site might become eight coordinated (Fig. 7). In that case the coordination of the A-site can be described as a square antiprism.

The X-site has a significantly larger scatter (50.2 e^-) than for a pure Sr-site, which is caused by Ba predominant in the site, with minor Sr and *REE* (Table 8). The Y-site is fully occupied by *REE* of which Ce is dominant. The incorporation of Ba for Sr at the X-site also results in an increase of the average bond distance of this site from 2.620 Å in nordite-(Ce) to 2.701 Å in illoqite-(Ce) (Table 8). It is somewhat surprising that the nordite structure can accommodate Ba as in previous studies the site contained not more than 5% Ba (e.g. Sokolova *et al.*, 1992; Pekov *et al.*, 1998, 2001). The only major substituent for Sr reported so far

Table 10. Bond-valence sums (vu) for illoqite-(Ce).

	A	B	X	Y	Z	T1	T2	T3	Σ
O1	0.093	0.201 ×2↓				0.905		0.940	2.14
O2	0.165		0.314 ×2↓		0.480 ×2↓	1.061			2.02
O3		0.120 ×2↓	0.195 ×2↓			0.855		0.938	2.11
O4	0.183	0.257 ×2↓	0.283 ×2↓			1.126			1.85
O5	0.101 ×2→						0.951 ×2→		2.11
O6	0.141			0.398 ×2↓	0.450 ×2↓		1.013		2.00
O7				0.196 ×2↓			0.872	0.938	2.01
O8	0.195			0.382 ×2↓			1.111		1.72
	0.029								
O9			0.318 ×2↓	0.431 ×2↓				1.103	1.85
Σ	0.91	1.16	2.22	2.81	1.86	3.95	3.95	3.92	

Note: bond-valence parameters are recalculated according to the site occupancies (see Table 8), and taken from Brown and Altermatt (1985) for all the cations apart from Si and *REE* for which the parameters from Gagné and Hawthorne (2015) have been used.

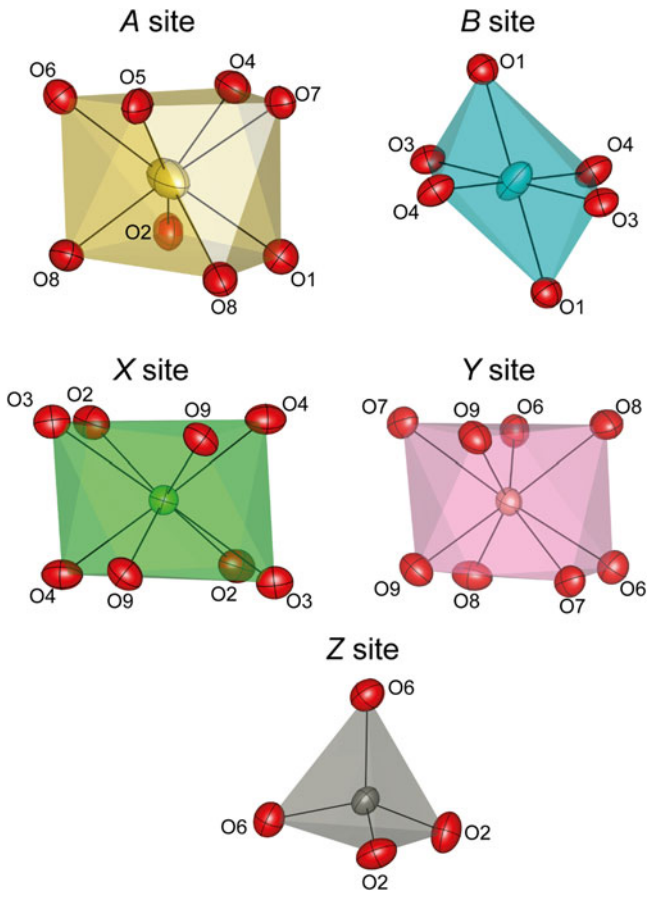

Fig. 7. View of the coordination around the crystallographic $^{[7+1]}$A, $^{[6]}$B, $^{[8]}$X, $^{[8]}$Y and $^{[4]}$Z sites in the structure of illoqite-(Ce). The displacement ellipsoids represent the 90% probability level.

has been Ca (e.g. Bakakin *et al.*, 1970; Dal Bo *et al.*, 2021) suggesting that the nordite structure is more flexible when it comes to incorporating smaller cations than larger cations at the X-site. However, the discovery of illoqite-(Ce) shows that this is not the case. Both the X and Y-sites show regular square antiprism coordination (Fig. 7).

The tetrahedrally coordinated Z-site is dominated by Zn, but has significant Fe, suggesting an iron dominant equivalent may exist. Generally, all the main cation sites have slightly larger average bond distances in illoqite-(Ce) compared to nordite-(Ce), which in turn is shown in a unit cell volume increase from 1472 to 1507 Å^3. The bond-valence calculations in accordance with the cationic distribution are presented in Table 10 and show only minor deviations from ideal values. Contrary to other nordite-supergroup minerals, illoqite-(Ce) also has Li as a monovalent cation in the Z-site. The average bond distance of the site is 1.973 Å which is very close to the ideal 1.96 Å for tetrahedrally coordinated Li (Wenger and Armbruster, 1991). Although only a few Li minerals are known from Ilímaussaq, polylithionite occurs in parts of the ussingite vein hosting illoqite-(Ce).

Acknowledgements. We appreciate assistance from Minik Jeremiassen from the Language Secretariat of Greenland to confirm the correct meaning of illoq. We wish to thank Associate Editor Ferdinando Bosi for handling the manuscript as well as the comments from reviewers Peter Leverett, Peter Bačik and Adam Pieczka.

Supplementary material. To view supplementary material for this article, please visit https://doi.org/10.1180/mgm.2021.104

References

Bakakin V.V., Belov N.V., Borisov S.V. and Solovyeva L.P. (1970) The crystal structure of nordite and its relationship to melilite and datolite–gadolinite. *American Mineralogist*, **55**, 1167–1181.

Bayliss P. and Levinson A.A. (1988) A system of nomenclature for rare-earth mineral species: revision and extenstion. *American Mineralogist*, **73**, 422–423.

Borst A.M., Waight T.E., Finch A.A., Storey M. and Le Roux P.J. (2019) Dating agpaitic rocks: a multi-system (U/Pb, Sm/Nd, Rb/Sr and ^{40}Ar/^{39}Ar) isotope study of layered nepheline syeneits from the Ilímaussaq complex, Greenland. *Lithos*, **324–325**, 74–88.

Brown I.D. and Altermatt D. (1985) Bond-valence parameters obtained from a systematic analysis of the Inorganic Crystal Structure Database. *Acta Crystallographica*, **B41**, 244–247 [with updated parameters from http://www.ccp14.ac.uk/ccp/web-mirrors/i_d_brown/].

Dal Bo F., Gulbransen E.H. and Friis H. (2021) New data on nordite-(Ce) and establishment of the nordite supergroup. *Mineralogical Magazine*, **85**, 431–437.

Engell J., Hansen J., Jensen M., Kunzendorf H. and Løvborg L. (1971) Berylium mineralization in the Ilímaussaq intrusion, South Grennland, with description of a field beryllometer and chemical methods. *The Geological Survey of Greenland*, **33**, 1–40.

Farrugia L.J. (2012) WinGX and ORTEP for Windows: and update. *Journal of Applied Crystallography*, **45**, 849–854.

Friis H. 2015. Primary and secondary mineralogy of the Ilímaussaq alkaline complex, South Greenland. Pp. 83–89 in: *Symposium on Strategic and Critical Materials Proceedings November 13–14, 2015 Victoria, British Columbia* (Simandl G.J. and Neetz M., editors). British Columbia Geological Survey Paper 2015-3.

Gagné O.C. and Hawthorne F.C. (2015) Comprehensive derivation of bond-valence parameters for ion pairs involving oxygen. *Acta Crystallographica*, **B71**, 562–578.

Gerasimovsky V.I. (1941) Nordite, a new mineral of the Lovozero tundra. *Doklady Akademii Nauk SSSR*, **32**, 496–498.

Griffin W.L., Powell W.J., Pearson N.J. and O'Reilly S.Y. (2008) Glitter: Data reduction software for laser ablation ICP-MS. Pp. 308–311 in: *Laser Ablation ICPMS in the Earth Sciences: Current practices and outstanding issues* (P. Sylvester, Editor). Mineralogical Association of Canada Short Course Series, 40.

Gulbransen E.H., Dal Bo F., Erambert M.M.L. and Friis H. (2021) Illoqite-(Ce), IMA 2021-021. CNMNC Newsletter 62; *Mineralogical Magazine*, **85**, https://doi.org/10.1180/mgm.2021.62

Hatert F. and Burke A.J. (2008) The IMA-CNMNC dominant-constituent rule revisited and extended. *The Canadian Mineralogist*, **64**, 717–728.

Holland T.J.B. and Redfern S.A.T. (1997) Unit cell refinement from powder diffraction data: the use of regression diagnostics. *Mineralogical Magazine*, **61**, 65–77.

Jarosewich E. and Boatner L.A. (1991) Rare-earth element reference samples for electron microprobe analysis. *Geostandards Newsletter*, **15**, 397–399.

Khomyakov A.P. (1995) *Mineralogy of hyperagpaitic alkaline rocks*. Oxford: Clarendon Press.

Larsen L.M. and Sørensen H. (1987) The Ilímaussaq intrusion – progressive crystallization and formation of layering in an agpaitic magma. *Geological Society, London, Special Publications*, **30**, 473–488.

Mandarino J.A. (1981) The Gladstone-Dale relationship: part IV. The compatibility concept and its application. *The Canadian Mineralogist*, **19**, 441–450.

Momma K. and Izumi F. (2011) VESTA 3 for three-dimensional visualization of crystals, volumetric and morphology data. *Journal of Applied Crystallography*, **44**, 1272–1276.

Pekov I.V. (2000) *Lovozero Massif, History, Pegmatites, Minerals*. Ocean Pictures Ltd., Moscow.

Pekov I.V Chukanov N.V., Kononkova N.N., Belakovsky D.I., Pushcharovsky D. Yu. and Vinogradova S.A. (1998) Ferronordite-(Ce) $Na_3SrFeSi_6O_{17}$ and manganonordite-(Ce) $Na_3SrMnSi_6O_{17}$ – two new minerals from Lovozero massif, Kola Peninsula. *Zapiski Vserossijskogo Mineralogicheskogo Obshchestva*, **127**, 32–41.

Pekov I.V., Chukanov N.V., Turchkova A.G. and Grishin V.G. (2001) Ferronordite-(La), $Na_3Sr(La,Ce)FeSi_6O_{17}$, a new mineral of the nordite group from Lovozero Massif, Kola. *Zapiski Vserossijskogo Mineralogicheskogo Obshchestva*, **130**, 32–41.

Petersen O.V. (2001) List of all minerals identified in the Ilímaussaq alkaline complex, South Greenland. *Geology of Greenland Survey Bulletin*, **190**, 25–33.

Pouchou J.L. and Pichoir F. (1984) A new model for quantitative X-ray microanalysis. I. Application to the analysis of homogeneous samples. *La Recherche Aérospatiale*, **3**, 13–38.

Pushcharovskii D.Y., Pekov I.V., Pluth J.J., Smith J., Ferraris G., Vinogradova S.A., Arakcheeva A.V., Soboleva S.V. and Semenov E.I. (1999) Raite, manganonordite-(Ce), and ferronordite-(Ce) from the Lovozero massif: Crystal structures and mineralogical geochemistry. *Crystallography Reports*, **44**, 565–574.

Semenov E.I. (1961) New data on nordite. *Trudy Mineralogicheskogo Muzeya, Akademiya Nauk SSSR*, **11**, 199–201.

Shannon R.D. (1976) Revised effective ionic radii and systematic studies of interatomic distances in halides and chalcogenides. *Acta Crystallographica*, **A32**, 751–767.

Sheldrick G.M. (2008) A short history of SHELX. *Acta Crystallographica*, **A64**, 112–122.

Sokolova E.V., Kabalov Y.K. and Khomyakov A.P. (1992) Isomorphism in the crystal structure of the Khibiny nordite, $Na_3SrTR\{M^{2+}[Si_6O_{17}]\}$, TR = La, Ce, Nd, Pr; M^{2+} = Zn, Mg, Fe, Mn (in Russian). *Vestnik Moskovskogo Gosudarstvennogo Universiteta*, **4**, 97–102.

Sørensen H. and Larsen L.M. (1987) Layering in the Ilímaussaq alkaline intrusion, South Greenland. Pp. 1–28 in: *Origins of Igneous Layering*. Springer, Dordrecht, The Netherlands.

Sørensen H. and Larsen L.M. (2001) The hyper-agpaitic stage in the evolution of the Ilímaussaq alkaline complex, South Greenland. *Geology of Greenland Survey Bulletin*, **190**, 83–94.

Upton B. (2013) Tectono-magmatic evolution of the younger Gardar southern rift, South Greenland. *Geological Survey of Denmark and Greenland Bulletin*, **29**.

Ussing N.V. (1912) Geology of the country around Julianehaab, Greenland, *Meddelser om Grønland*, **38**, 1–426.

Wenger M. and Armbruster T. (1991) Crystal chemistry of lithium: oxygen coordination and bonding. *European Journal of Mineralogy*, **3**, 387–399.

Yang H., Gu X., Downs R.T., Evans S.H., Van Nieuwenhuizen J.J., Lavinsky R.M. and Xie. X. (2019) Meieranite, $Na_2Sr_3MgSi_6O_{17}$, a new mineral from the Wessels mine, Kalahari manganese fields, South Africa. *The Canadian Mineralogist*, **57**, 457–466.